

Power Loss Distribution And Characterization Of Modular Multilevel Converter For Smart Grid Applications

Fazal Muhammad *, Haroon Rasheed*

*Department of Electrical Engineering, Bahria University Karachi Campus, 13, National Stadium Road, Karachi, Pakistan

(Fazalkhan00@gmail.com, Haroonrasheed.bukc@bahria.edu.pk)

‡ Corresponding Author; Fazal Muhammad, 13, National Stadium Road, Karachi, Pakistan, Tel: +923328068744,
fazalkhan00@gmail.com

Received: 12.05.2022 Accepted: 13.06.2022

Abstract- The efficiency of the Module multilevel converter (MMC) is strongly dependent on the on-state conduction and switching power losses of the semiconductors of its submodules. The conduction power losses of the submodule of an MMC depend on the load current, duty cycle, and power factor whereas switching power losses depend on switching frequency, dc-link voltages, and load current. It is nevertheless crucial to take into account the influence of converter operating points on the overall system efficiency in order to determine an accurate estimate of semiconductor losses in the submodule. In this paper, we evaluate the on-state power loss characteristics of a submodule when it is subjected to changes in the switching frequency, modulation index, and power factor. The power losses of MMC have been presented for the four-quadrant operations i.e. inverter (inductive), rectifier (inductive), rectifier (capacitive), and inverter (capacitive). The evaluation of the power losses has been carried out employing PLECS[®] to examine the losses of the MMC.

Keywords MMC, Steady-state power losses, IGBT Losses, Switching power loss, Freewheeling diode, Voltage source converter.

1. Introduction

Power grid systems use voltage source converters (VSC) for converting AC - DC and DC - AC power. The advantages that have been claimed for VSC technology are their smaller site foot-mark, capability to feed the passive loads, and control of the reactive and active power. Voltage source converters that are used in commercial service are based on 2-level, 3-level, and 5-level converters [1]. The operation of these converters relies on comparatively higher switching frequencies, typically 1-2 kHz, for switching of IGBTs to suppress the higher contents of harmonic distortion [2]. However, the switching frequencies in this range lead to higher switching losses in the IGBTs' transistor and anti-parallel diodes of the converter [3]. VSC has relatively higher steady-state power losses than that of the thyristor-based line commutated converters (LCCs) [4], [5]. The power losses of the VSC are in the range of 2% - 4%, excluding the line or cable losses. These power losses of VSC are higher than that of the LCC's power losses, which are about 0.75 %. Higher power losses and harmonic distortion of the VSC have reduced the conversion efficiency of the converter when interfaced with the electrical grid system [6]. Recent developments in power electronics have greatly benefited the use of modern converters in many industrial applications. The modular structure of the voltage source converter has dramatically

changed this scenario. Modular multilevel converters are well-established advanced technology first introduced in 2001 [7]. It has promising features for use in medium/high voltage applications. Implementation of this technology has several advantages, including voltage scalability, increased reliability, reduced harmonic distortion, low power losses, and better efficiency [8], [9]. The growing popularity of MMC is due to their lower total harmonic distortion (THD), fault tolerance, redundancy [10], [11], [12] higher quality of output voltage, low power losses in their semiconductor switches, and reduced size of their filters [13], [14]. It is an ideal converter for electric railways and also applicable for industrial motors because of its capability of extending several hundred voltage levels, as well as high-voltage transmission networks [15], [16]. Modular multilevel convert has the capability of the DC and AC fault ride-through capabilities to reduce the cost of the DC circuit breakers [17]. MMC is also a potential converter to deal the power quality problems such as voltage sag and swell mitigation. All these factors allow it a promising future in medium and high voltage AC and DC network systems such as large wind turbines and AC and DC transmission networks. However, although the modular multilevel converter is gaining a new competitive position in the field of energy transmission, one of the most critical aspects turns out to be the power losses of this converter.

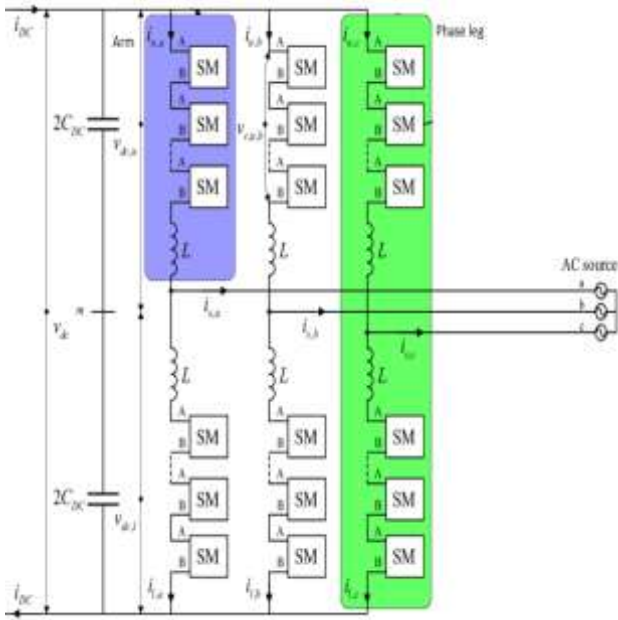


Fig. 1. Three-phase Modular multilevel converter.

Three-phase MMC is shown in fig 1. Each phase of it has the same number of submodules and an inductor “L” is in series with both the lower and upper arms. Each submodule consists of IGBTs, free-wheeling diodes, and series loop capacitors, which do not consume energy during the charging and discharging process but it is energy storage components [18]. Therefore, the power losses of the modular multilevel converter are the power losses of insulated-gate bipolar transistors (IGBTs) and free-wheeling diodes (FWDs) of submodules i.e. on-state conduction power loss of IGBT, free-wheeling diode, switching power losses of IGBT and reverse recovery power loss of anti-parallel diode.

1.1 Contributions

- This paper examines the power loss of semiconductor devices within the submodule of MMC.
- The losses of the IGBT module and the free-wheeling diode is analyzed when switching frequency, modulation index, and the power factor are changed.
- The power losses of MMC have been examined for the four-quadrant operations i.e. inverter (inductive), rectifier (inductive), rectifier (capacitive), and inverter (capacitive).

2. Power Losses Evaluation

In literature, several methods have been proposed to estimate the power losses of semiconductors [19],[20]. However, these methods are computationally intensive when applied to a large number of SMs, as is typically the case with MMCs. The methodology used in this research article is carried out using PLECS®, a simulation platform for power electronics systems. First, the complex structure of the modular multilevel converter has been designed, taking into account

the parameters of table 1. The evaluation of the power losses has been carried out employing specific block diagrams present in the PLECS® library. The modular multilevel converter has therefore been able to evaluate the conduction and switching losses associated with the switching devices. Calculating the losses generated depends on which semiconductor device is adopted. It is proposed that the MMC would be more robust if it were composed of IGBTs operating at 3.3 kV blocking voltage. Therefore, the ABB-5SNA 1500E330305 (3.3 kV/1.5 kA chip) appears to be a viable option to quantify the losses incurred because of MMC.

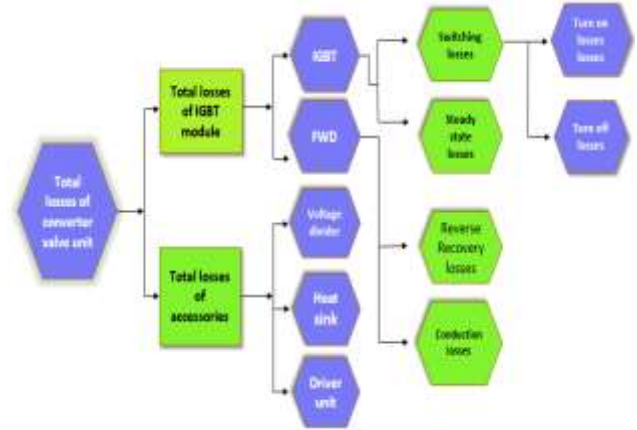


Fig. 2. Power losses classification of a cell of Modular Multilevel Converter.

2.1 Categories Of Submodules Losses

The submodule losses can be divided into the following categories:

- Conduction losses of IGBT.
- Conduction losses of the diode.
- Conduction losses of submodule.
- Switching losses of the IGBT.
- Turn-on/switching losses of the diode.
- Switching losses of the submodule.
- Snubber losses.

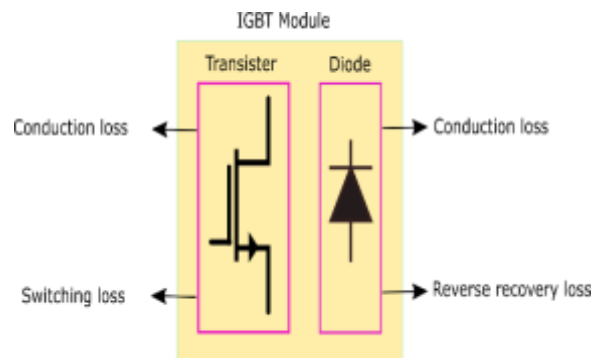


Fig. 3. Loss distribution of IGBT.

The main loss of power during semiconductor device operation is due to conduction and switching losses [21]. In

submodules with a snubber circuit, snubber losses can be quite high, but MMC submodules usually do not use them [22]. Therefore, they can be neglected. Other losses that should be considered in a modular multilevel Converter are:

- Ohmic losses of an arm inductor.
- Losses of the cooling system.

These losses will be analyzed summarily.

2.2 IGBT Power Losses

IGBT modules suffer conduction loss and switching loss during operation. Conduction power losses depend on both the converter load current and duty cycle while switching power losses depend on junction temperature, load current, and dc-link voltages.

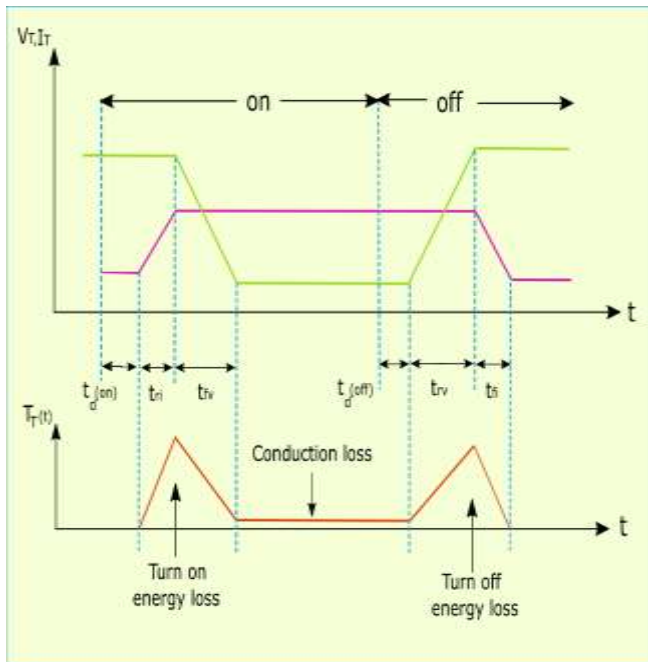


Fig. 4. Switching characteristics of IGBT.

An increase in junction temperature is being a critical situation for the converter, so it needs a suitable heat sink system for protection. The switching characteristics of the IGBT module are illustrated in Fig 4, which illustrates the voltage, current, and power losses when the power is turned on and turned off. Fig 3 illustrates the power loss distribution of the IGBT module. The operation time during turn-on and turn-off of the switch is divided into delay t_d rise time t_{ri} and fall time respectively. During both the turn-on and turn-off phases, a delay time t_d is absorbed during the practical operation. During the switching operation, current rises, t_{ri} is current rise time, from zero point to a specific point whereas voltage falls is represented by t_{fv} . The same can be seen during the off operation time of the switch. In an IGBT module, switching power loss is represented by the following equation.

$$E_{sw} = E_{on} + E_{off} \tag{1}$$

Where, E_{on} is a turn-on and E_{off} is turn-off energy losses of the IGBT module. The total conduction power loss of the IGBT module can be calculated by the following equation

$$P_{Cond(Total)} = P_{Cond(IGBT)} + P_{Cond(Diode)} \tag{2}$$

2.3 Conduction Loss

In the on-state or active condition of a submodule of the converter, both the transistor and free-wheeling diode of the IGBT of a submodule have power losses. Current times of the voltage drop are measured as the power dissipation and conduction current with a constant voltage drop. As a result of the conduction period, power is dissipated by the resistive element based on RMS current squared times the resistance. The following equation can be used to calculate IGBT conduction losses within a submodule of a converter.

$$P_{Cond(IGBT)} = V_{on} \cdot I_{avg} + R_c \cdot I_{rms}^2 \tag{3}$$

Type ABB- 5SNA 1500E330305 module is used as a switch of submodules of converter where V_{on} is the on-state voltage of IGBT and its value is taken from typical on-state characteristics, I_p is the peak current, ABB-5SNA1500E330305 has typical output characteristics in which R_c is the on-state resistance found by dividing the change in voltage over the change in current, m_a is the modulation index, \cos is the power factor and for I_{rms} , integrate the current square duty cycle and take the square root of the result.

$$I_{avg} = I_p \left(\frac{1}{2\pi} + \frac{m_a \cdot \cos\theta}{8} \right) \tag{4}$$

$$I_{rms} = I_p \sqrt{\frac{1}{8} - \frac{m_a \cdot \cos\theta}{3\pi}} \tag{5}$$

We can calculate IGBT's conduction power losses, switching losses, and conduction power losses of free-wheeling diode based on switching and on-state characteristics given in the datasheet of ABB- 5SNA 1500E330305 module. Based on the diode forward characteristic, R_d can be calculated by dividing the change in voltage by the change in current. The mathematical equation for calculation of conduction power loss of diode is given by

$$\begin{cases} P_{Cond(Diode)} = V_d \cdot I_{avg} + R_d \cdot I_{rms}^2 \\ I_{avg} = I_p \left(\frac{1}{2\pi} + \frac{m_a \cdot \cos\theta}{8} \right) \\ I_{rms} = I_p \sqrt{\frac{1}{8} - \frac{m_a \cdot \cos\theta}{3\pi}} \end{cases} \tag{6}$$

2.4 Switching Power Loss

Switching power losses occurs during on and off intervals of the device. The turn-on and turn-off energy losses of IGBT can be calculated from the following mathematical equations. The values of turn-off switching energy E_{off} , nominal voltage V_{nom} , turn-on switching energy E_{on} , nominal current I_{nom} , $t_{c(on)}$, $t_{c(off)}$ switching energies per pulse against collector current, current fall time, and typical switching times V_s collector

current can be found from data-sheet of IGBT given in datasheet of IGBT.

$$\left\{ \begin{array}{l} E_{on} = \frac{1}{2} V_{nom} I_p t_{c(on)} \\ E_{off} = \frac{1}{2} V_{nom} I_p t_{c(off)} \\ E_{Total} = Kg(E_{on} + E_{off}) \cdot \frac{V \cdot I}{V_{nom} \cdot I_{nom}} \end{array} \right. \quad (7)$$

Where $t_{c(on)}$ and $t_{c(off)}$ are

$$\begin{aligned} t_{c(on)} &= t_{ri} + t_{fv} \\ t_{c(off)} &= t_{rv} + t_{fi} \end{aligned}$$

the values of E_{on} (turn-on switching energy), E_{off} (turn-off switching energy), nominal voltage V_{nom} , nominal current I_{nom} , $t_{c(on)}$, $t_{c(off)}$ switching energies per pulse against collector current, current fall time, and typical switching times Vs collector current can be found from data-sheet of IGBT given in datasheet of IGBT. The correction factor is Kg and its value can be considered 1.1-1.2. Total energy loss due to switching can be calculated by

$$E_{Total} = Kg(E_{on} + E_{off}) \cdot \left(\frac{V \cdot I}{V_{nom} \cdot I_{nom}} \right) \quad (8)$$

The product of energy loss and switching frequency throughout $\frac{2}{\pi}$ is power loss which is given by

$$P_{swit(IGBT)} = \frac{E_{Total}}{\pi} \cdot f_s \quad (9)$$

2.5 Reverse Recovery Power Loss of The Diode

Power loss occurs in the free-wheeling diode of IGBT of the submodule of the converter due to reverse recovery. The time during which the diode stops current to flow through it is known as the reverse recovery time (RRT) of the diode. The time is needed to discharge the diode and reverse recovery losses that occur during this period is

$$E_{Recovry(Diode)} = E_{Rec(given)} \cdot \left(\frac{V \cdot I}{V_{nom} \cdot I_{nom}} \right) \quad (10)$$

Where V is the operating voltage across each switch and I is the peak current value of the operating current. The power loss of the reverse recovery of the diode can be found in the equation

$$P_{Rec(Diode)} = \frac{E_{Recovry(Diode)}}{\pi} \cdot f_s \quad (11)$$

2.6 The Total Power Loss of A Cell

Total power losses of the converter's cell are the total power losses of IGBTs in a cell and losses of the free-wheeling diode. Each cell of the converter is composed of IGBTs and anti-parallel free-wheeling diodes. The losses of IGBT and anti-parallel free-wheeling diode of a cell of MMC also depend on the system's power factor, modulation index of the converter, and their switching frequencies. In this article, section simulation, the losses have been simulated only for one submodule and the results are multiplied by the total number of submodules, reducing the total simulation time and obtaining a good accuracy of results.

2.7 Additional Losses

The additional power losses of the MMC are given below

2.7.1 Ohmic losses of an arm inductor:- The ohmic losses of an arm inductor, also called the outdoor air-core reactor, of the MMC, are given by

$$P_{ind} = R_{ind}^{\theta} - I_{arm,rms}^2 \quad (12)$$

Here R_{ind}^{θ} is the AC and DC resistance of the inductor of the MMC at θ° C and $I_{(arm,rms)}$ is the arm current of the MMC.

- *Losses of the cooling system:* Since large converters use a complex cooling system to properly carry out their operation, it is necessary to take into account also the losses generated by this cooling system. Pumps and heat exchangers are used to increase the reliability of the converter and to provide it with good electrical isolation. The evaluation of these losses is not quite simple. Using the coefficient of performance of the cooling system is one way to determine its performance. The COP measures the heat extracted over the power needed to carry out this extraction.

2.7.2 The Total Power Loss of MMC

Assuming that the number of submodules in the upper arm of an MMC is H and in the lower arm is L. Where N is the sum of the total number of the sub-modules per phase of MMC in the lower and upper arms is given by

$$N = H + L \quad (13)$$

Therefore, according to equations 2, 9, and 11, the total power losses of the modular multilevel converter per phase is P_{TOTAL} given by

$$P_{Total} = [H \cdot (P_{cond(IGBT)} + P_{cond(Diode)}) + L \cdot (P_{cond(IGBT)} + P_{cond(Diode)}) + N \cdot (P_{swit(IGBT)} + P_{Rec(Diode)})] \quad (14)$$

For the three-phase system, the total loss power losses of MMC is P_{TOTAL} given by

$$P_{Total} = 3 \cdot [H \cdot (P_{cond(IGBT)} + P_{cond(Diode)}) + L \cdot (P_{cond(IGBT)} + P_{cond(Diode)}) + N \cdot (P_{swit(IGBT)} + P_{Rec(Diode)})] \quad (15)$$

2.8 Analysis of the Loss Characteristics of the Cell Of MMC

The theoretical analysis for conduction and switching power losses of the IGBT and diode of a submodule is as follows

- Loss characteristics of the IGBT and diode of a submodule of MMC when the switching frequency of the system is changed.
- Loss characteristics of the IGBT and diode of a submodule of MMC when the modulation index is changed.
- Loss characteristics of the IGBT and diode of a submodule of MMC when the power factor of the system is changed.

2.9 Results of Analysis

The switching losses in a converter are mainly because of switching frequency. The switching losses occur in the transistor and diode of IGBT during the period of turn on and turn off. The main components of the switching losses of a cell of the converter are diode reverse recovery losses, IGBT turns on and turn off losses. Fig 5, shows that increase in the switching frequency of the cell's switches as per equations 10 and 11, switching losses of the IGBTs and reverse recovery power losses of its free-wheeling diode are also increased.

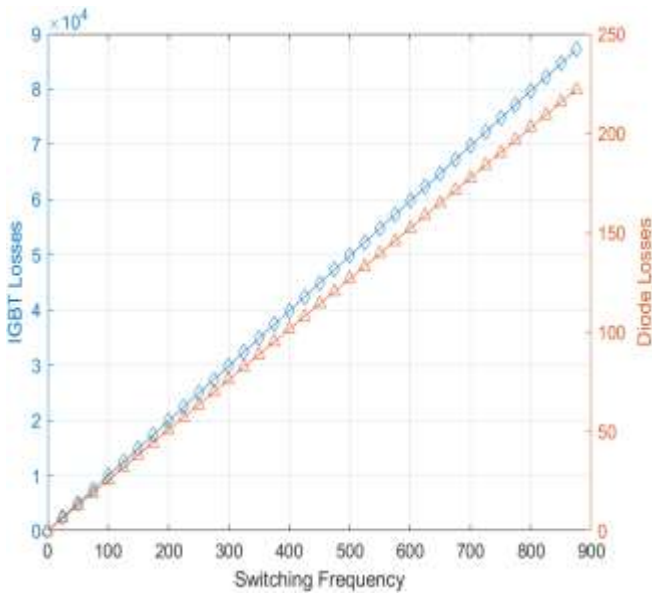


Fig. 5. Switching losses (W) of IGBT and diode (W) of a cell of the converter with changing switching frequency.

Though an increase in switching frequency stabilizes the power output of the converter and reduces the harmonic distortion it also increases the junction temperature which is not favorable for the converter. Similarly, Fig 6 is obtained while changing the modulation index as per equations 3 and 6 which shows the conduction losses of the IGBT and diode of a cell of the converter. An increase in the modulation index reduces the conduction power losses of the IGBT and diode of a cell.

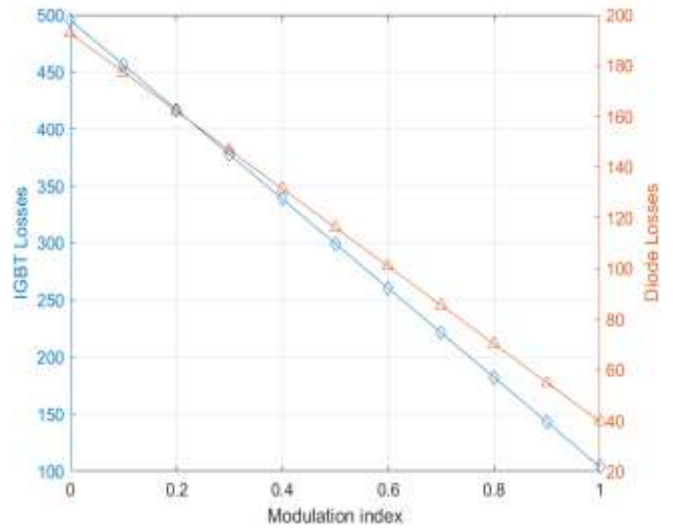


Fig. 6. Conduction losses (W) of IGBT diode (W) of a cell of the converter with changing modulation index.

Fig 7 shows the conduction power loss of the IGBT and free-wheeling diode of a cell of the converter. It is obtained while changing the load phase angle of the system as per equations 8 and 6. The conduction power loss of the IGBT and anti-parallel diode was reduced but the IGBT module has more power loss than that of the anti-parallel diode.

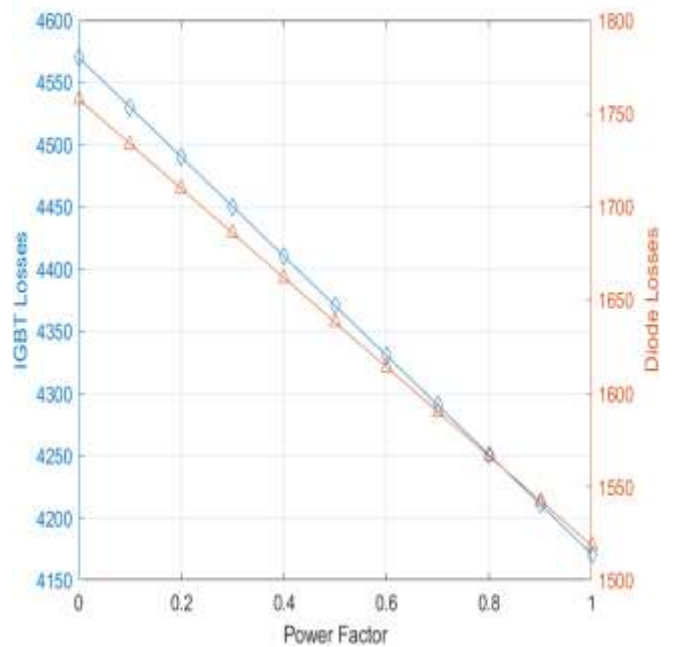


Fig. 7. Conduction losses (W) of IGBT and free-wheeling diode (W) of a cell of the converter with changing power factor.

3. Simulation Results

The simulation performed for power loss analysis of MMC is conducted in a PLECS® system. The switching and conduction losses of each device and their impact are evaluated over a broad range of active and reactive power flow combinations. The parameters of the IGBT module ABB-5SNA 1500E330305 and the system that has been used in the simulation are shown in table 1. The ambient temperature has

been defined as equal to 25⁰ C. The losses have been simulated only for one submodule and the results are multiplied by the total number of submodules, reducing the total simulation time and obtaining a good accuracy of results.

Table 1. Characteristic parameters of the MMC and power System.

Characteristic Parameter	Value	Unit
AC grid voltage	320	kV
Power factor	0.95	Capacitive
Rated power	526	MVA
Phase Reactor Impedance	J0.05	(p.u)
Arm Reactor Impedance	0.01+j0.2	(p.u)
Sub-module Capacitance	8	mF
Average Submodule voltage	1.6	kV

3.1 Possible States of the Submodule

The losses generated by a submodule depend on the direction of the arm current flowing through it and the state of the submodule of the converter. To evaluate the losses of the submodule, it is necessary to identify which device is involved and which device is in conduction mode at a given time instant. Four possible states have to be considered:

- *State I:* When the arm current is positive, D₁ conducts and current flows through the capacitor, charging it. However, when the arm current is negative, IGBT₁ conducts, and the capacitor discharges.
- *State II:* When the arm current is positive, IGBT₂ conducts, and the capacitor is bypassed. However,

when the arm current is negative, D₂ conducts, and the capacitor is also bypassed.

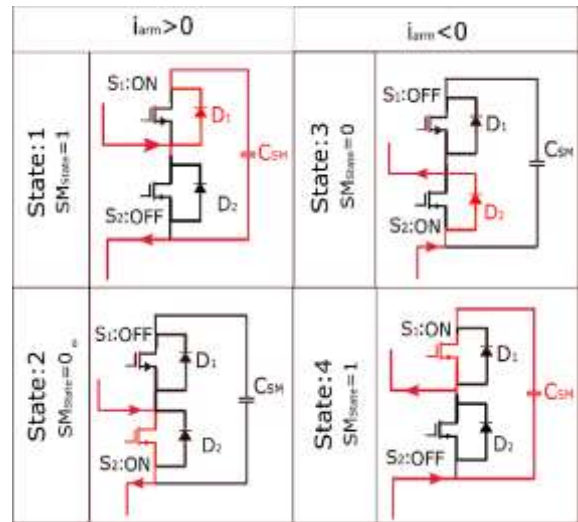


Fig. 8. Possible states of the submodule depend on the direction of the arm current.

The switching losses depend on the changes in the switching states of the submodule (from 0 to 1 and vice versa) and the direction of the arm current. When the arm current is positive and the SM state changes from 1 to 0, the diode D₁ stops conducting resulting in energy lost E_{rec} and the IGBT₂ starts conducting dissipating the energy E_{on}. Instead, if the SM state changes from 1 to 0, the IGBT₂ stops conducting dissipating the energy E_{off} and the diode D₁ starts conducting dissipating energy negligible. The same reasoning can be applied when the arm current is negative. In the Figures below, taking into account the arm upper current of phase a is shown the path of the current of each device involved for each submodule state. The simulations shown below are performed when P = 500 MW and Q = 0 MVAR.

- *When the arm current is positive*

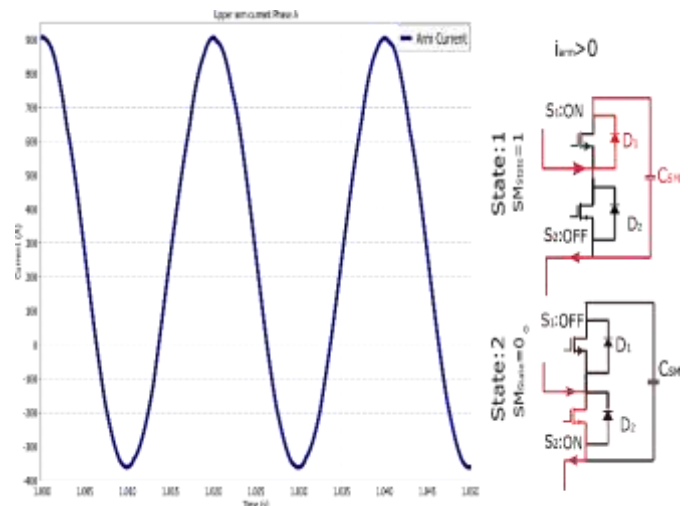


Fig. 9. Upper arm current and state of submodule with positive arm current.

When the direction of the current is positive; in state 1, S_1 is ON and S_2 is OFF, diode D_1 conducts, and the current flows through

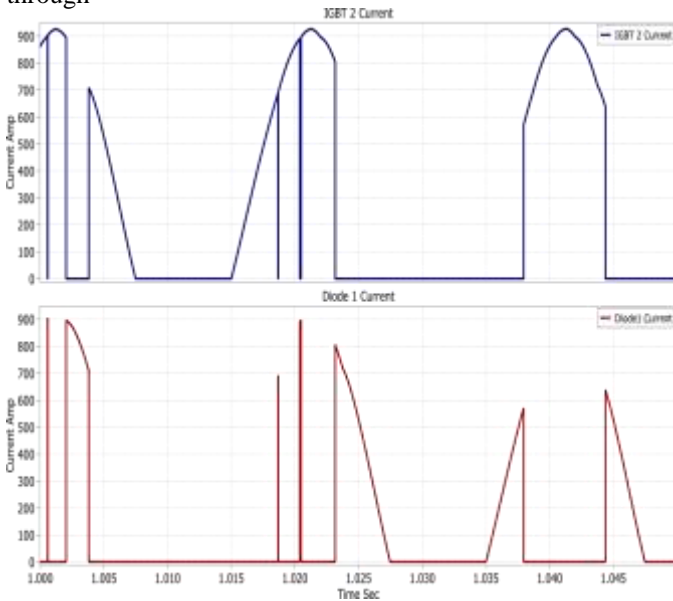


Fig. 10. IGBT-2 current, Diode-D1 current.

the capacitor of the submodule, consequently it charges the capacitor of the submodule. In-state 2, S_2 is ON and S_1 is OFF, the arm current flows through the IGBT₂ and the capacitor of the submodule is bypassed. Arm current and state of the submodule are illustrated in Fig 9 and Fig 10.

- When the arm current is negative

When the direction of the current is negative; in state 3, S_1 is OFF and S_2 is ON, diode D_2 conducts, the current flows through the anti-parallel D_2 and the capacitor of the submodule is bypassed.

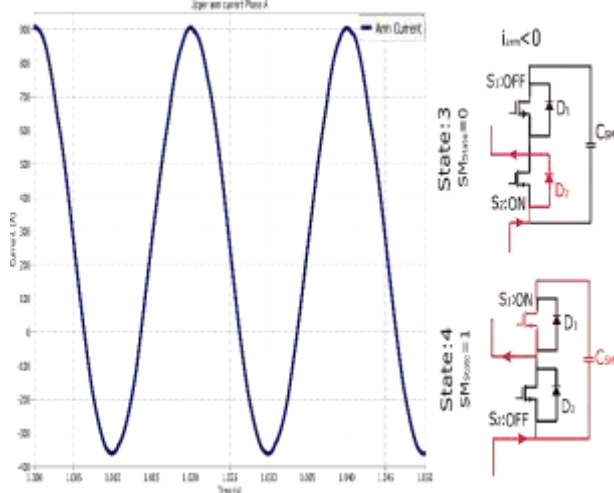


Fig. 11. Upper arm current and state of submodule with negative arm current.

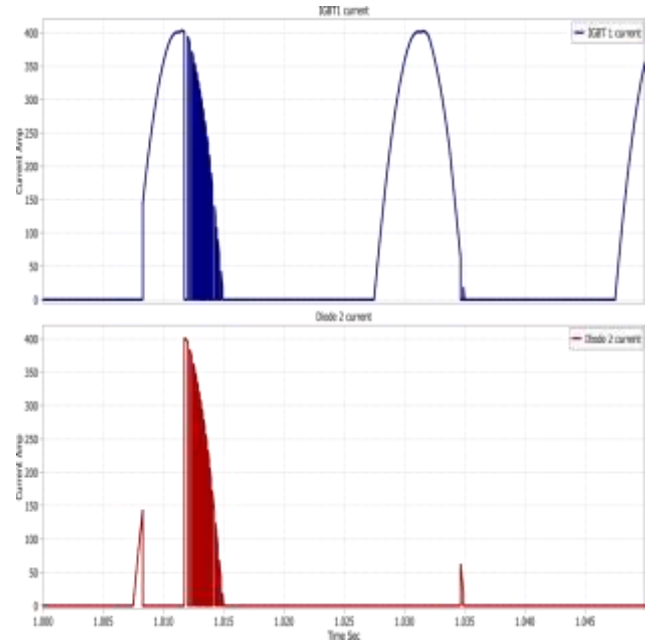


Fig. 12. IGBT₁ current and Diode₂ current.

In-state 4, S_1 is ON and S_2 is OFF, the arm current flows through the IGBT₁ and the capacitor of the submodule is charged. Arm current and state of the submodule are illustrated in Fig 11 and Fig 12.

3.1 Power Flow Simulations

The simulations are performed to analyze the conduction and switching power losses of the semiconductor devices of a submodule using PLECS®. The parameters of Table 6.1 and the IGBT module ABB- 5SNA 1500E330305 have been used in the simulations. Conduction power and switching losses of each semiconductor device and their impact are evaluated over a broad range of active and reactive power flow combinations.

- When $P = 500 \text{ MW}$ $Q = 0 \text{ MVAR}$

Fig 13, illustrates that the average conduction loss of the IGBT₂ and Diode₁ is more than that of the average conduction loss of IGBT₁ and Diode₂ respectively. When modular multilevel converter operates in inverter mode transferring active power of 500 megawatts from DC grid side to AC grid network. The conduction power losses of the semiconductor devices of the modular multilevel converter are simulated for analysis.

This is because when the direction of the current is positive IGBT₂ and Diode₁ conducts the arm current, so the conduction power losses of both are high.

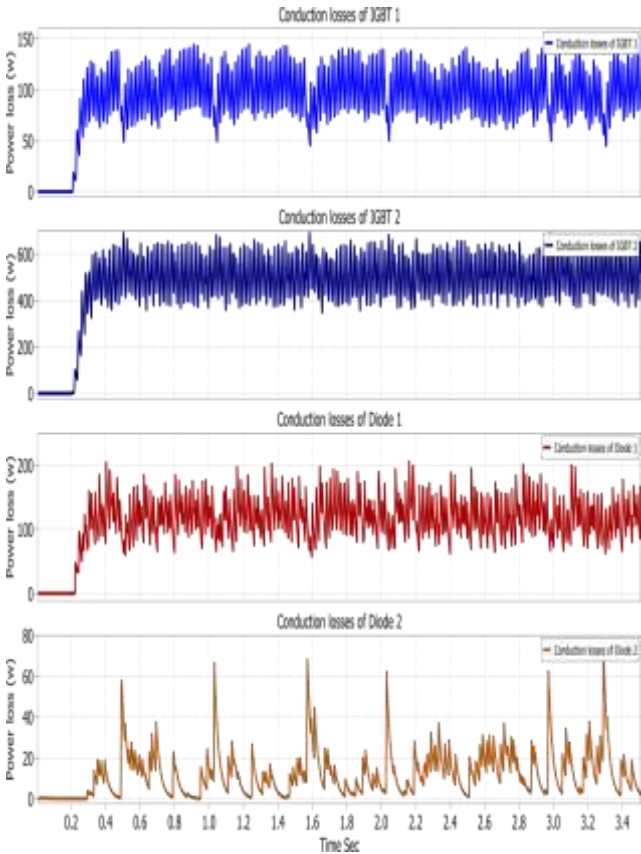


Fig. 13. The conduction power loss of IGBT₁, IGBT₂, Diode₁, and Diode₂.

The switching loss of the semiconductor devices of the modular multilevel converter is simulated for analysis. Fig 14, illustrates that the average switching loss of the IGBT₂ and Diode₁ is more than that of the average switching loss of IGBT₁ and Diode₂ respectively. This is because when the direction of the current is positive IGBT₂ and Diode₁ perform a switching function to conduct the arm current, so the switching power losses of both are high. The total power losses of the cell of MMC are illustrated in Fig 15. It is clear from the above figures that the contribution of conduction loss of the semiconductor devices is higher than that of switching losses.

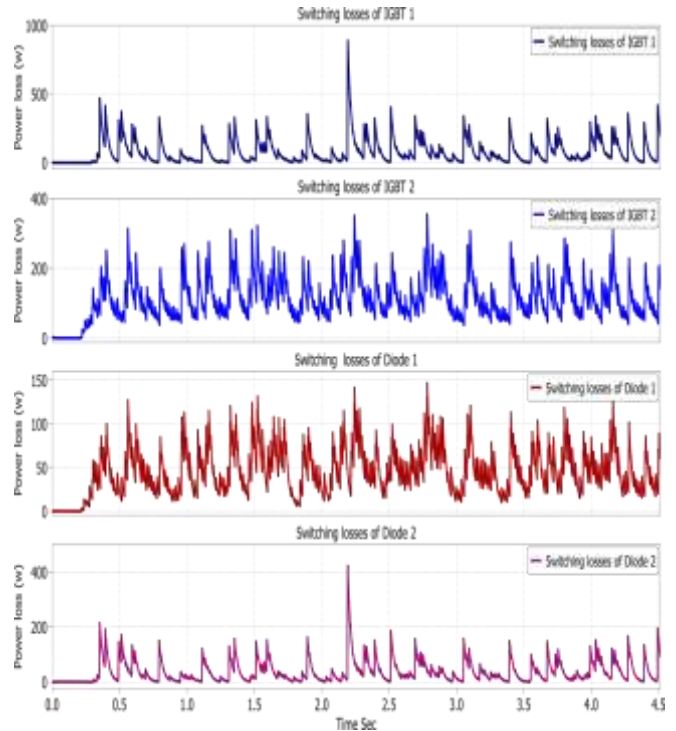


Fig. 14. Switching power loss of IGBT₁, IGBT₂, Diode₁, and Diode₂.

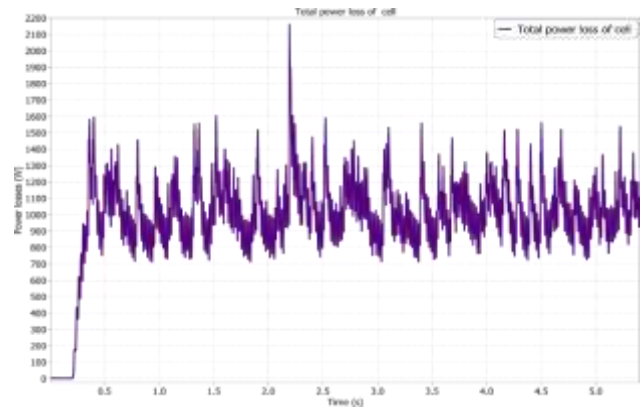


Fig. 15. The total power loss of a cell of MMC.

3.2 Active Power Flow Injection

In this section, we have studied and analyzed the conduction, switching, and overall power losses of the semiconductor devices of the cell of the MMC when different active power is injected.

- When active power (P) = 500 MW and Q=0 MVAR
- When active power (P) = 600 MW and Q=0 MVAR
- When active power (P) = 700 MW and Q=0 MVAR
- When active power (P) = 750 MW and Q=0 MVAR

The conduction power loss depends on the load current of the converter, duty cycle, and junction temperature whereas switching power losses depend on dc-link voltages, load current, and junction temperature. An increase in switching frequency makes the output voltage profile better and reduces

converter harmonics but it increases the switching power loss and junction temperature. An increase in junction temperature is being a critical situation for the converter, so it needs a suitable heat sink system for protection. Conduction power losses are dependent on load current; reduction of load current can be only possible if parallel conduction devices are provided. Parallel conduction devices can reduce steady-state power loss but their switching operation affects the overall efficiency of the converter. The conduction power loss of the MMC When the active power is $P= 500 \text{ MW}$, $P= 600 \text{ MW}$, $P= 700 \text{ MW}$, and $P= 750 \text{ MW}$, and reactive power is $Q=0 \text{ MVAR}$ respectively, the power loss of a submodule is calculated and presented to analyze the power losses of a cell of the modular multilevel converter. Fig 16, 17, 18, and Fig 19 illustrate the power losses of a submodule when different active power is injected.

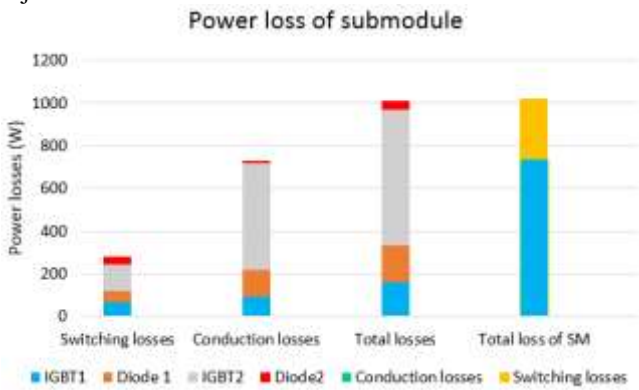


Fig. 16. The power loss of a submodule, Active power (P) =500 MW and reactive power (Q) =0 MVAR

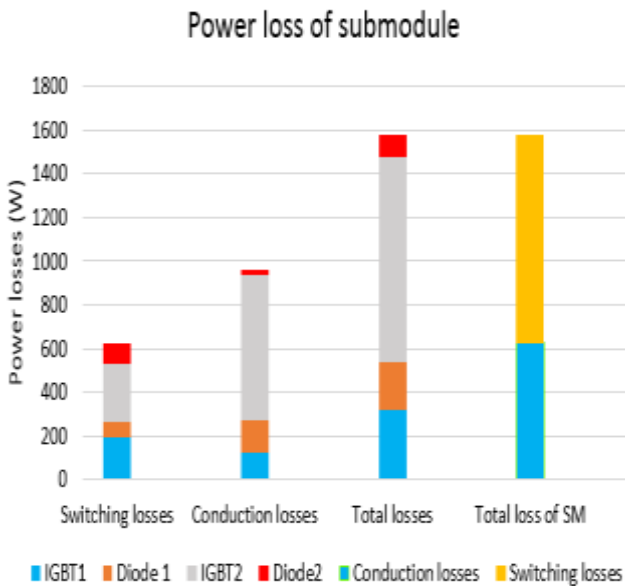


Fig. 17. The power loss of a submodule, Active power (P) =600 MW and reactive power (Q) =0 MVAR

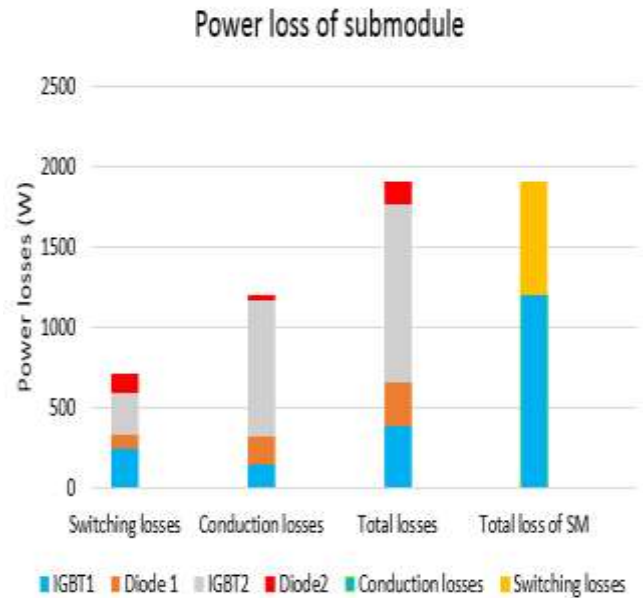


Fig. 18. The power loss of a submodule, Active power (P) =700 MW and reactive power (Q) =0 MVAR

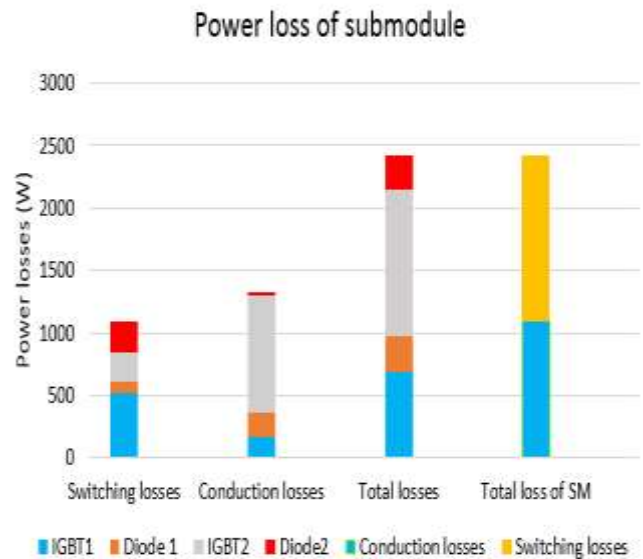


Fig. 19. The power loss of a submodule, Active power (P) =750 MW and reactive power (Q) =0 MVAR

3.3 Quadrant Operations and Power Loss

To analyze the losses of the converter, it has been examined for the four-quadrant operations. For power loss analysis both MMC-inverter and MMC-rectifier, leading and lagging power factors and mode of modular multilevel converter i.e. inverter (inductive), rectifier (inductive), rectifier (capacitive), and inverter (capacitive) have been considered. Various operations involve different converter losses. The power losses of the modular multilevel converter are illustrated in Fig 20, 21, 22, and 23 for different active and reactive power injections and all the four-quadrant operations. The most evident fact is that the various operations involve different converter losses.

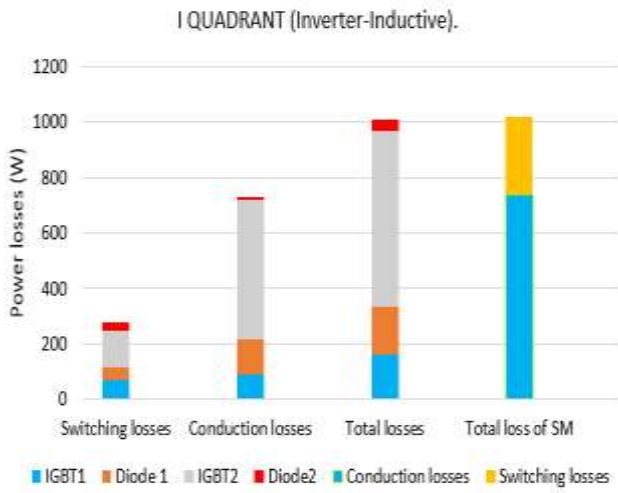


Fig. 20. Quadrant I, P = 500 MW, Q = 0 M VAR, PF= 1.

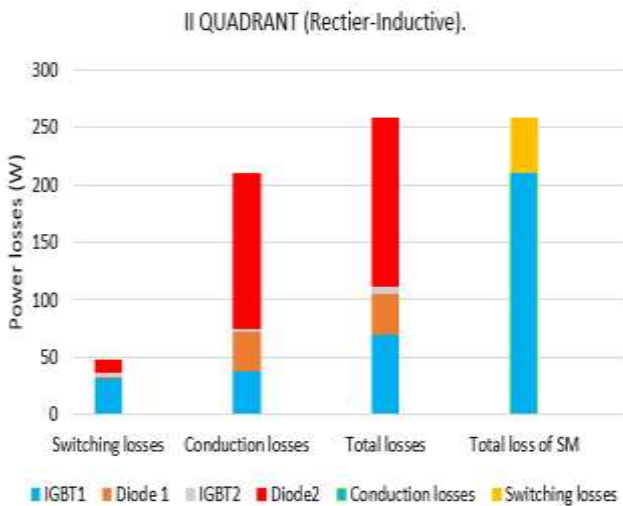


Fig. 21. Quadrant II, P = -201 MW, Q = 486 M VAR, PF = -0.38.

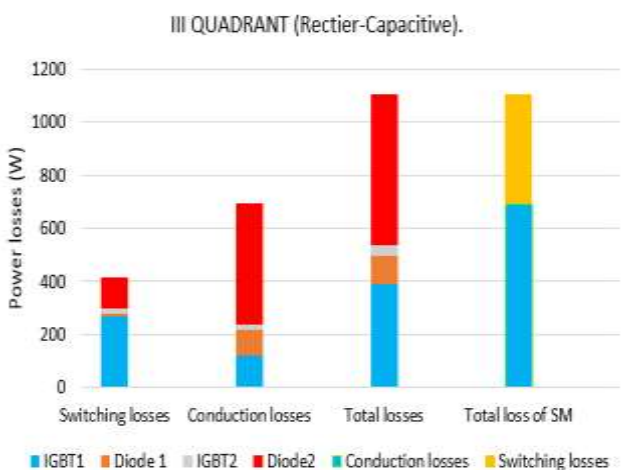


Fig. 22. Quadrant III, P = -486 MW, Q = -201 M VAR, PF = -0.38.

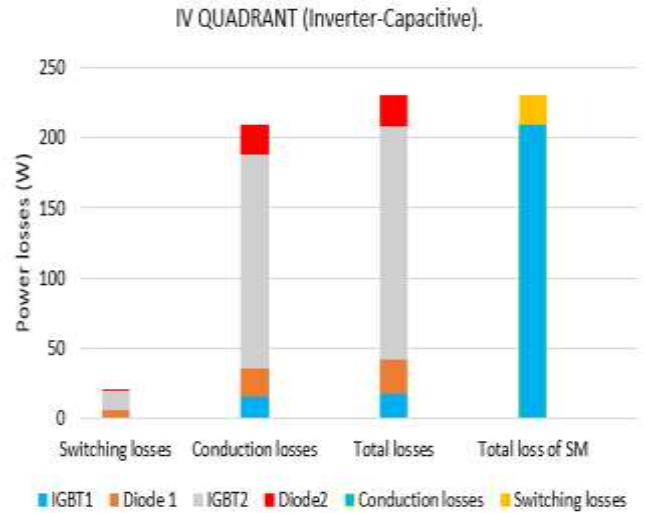


Fig. 23. Quadrant IV, P = -486 MW, Q = -201 M VAR, PF = 0.38.

The most evident fact is that the various operations involve different converter losses. Focusing on the inverter and rectifier modes keeping the reactive power equal to zero, the increase of the active power ow between the converter and its ac grid increases the ac and dc currents that flow on the converter arms. As a consequence, it increases the overall conduction losses that are being generated. In general, the losses generated in the inverter and rectifier modes are quite similar to each other, but it is possible to notice that if in the inverter mode the arm currents ow mainly in the IGBTs, in the rectifier mode the diodes are more stressed. As regards the reactive power flow injection, although the conduction losses turn out to be evenly distributed among the switching devices, the situation for the switching losses is different. The switching losses are strongly influenced by the reactive power injection. Increasing the reactive power injection increases the total power losses of the converter since the submodules are turned on more frequently. Moreover, there is a substantial difference between the capacitive reactive power injection and the inductive one. In the case of inductive reactive power ow between the converter and the ac grid, the switching losses are higher.

3.4 The Efficiency of the Converter

The conversion efficiency of the modular multilevel converter depends on the converter’s power loss. A modular multilevel converter has a higher conversion efficiency when the total power loss of the semiconductor devices inside the submodule of the modular multilevel converter is low. The efficiency of the MMC is the percentage ratio of the P_{OUT} to P_{in} . Where P_{loss} is the total power loss of the semiconductor devices of MMC. Total power loss and efficiency are calculated for a modular multilevel converter at different active power as shown in fig 24 and 25 receptively.

$$P_{in} = P_{out} + P_{loss} \tag{16}$$

The efficiency of the MMC converter is given by

$$\eta = \frac{P_{out}}{P_{in}} \cdot 100 = \frac{P_{out}}{P_{out} + P_{loss}} \cdot 100 \tag{17}$$

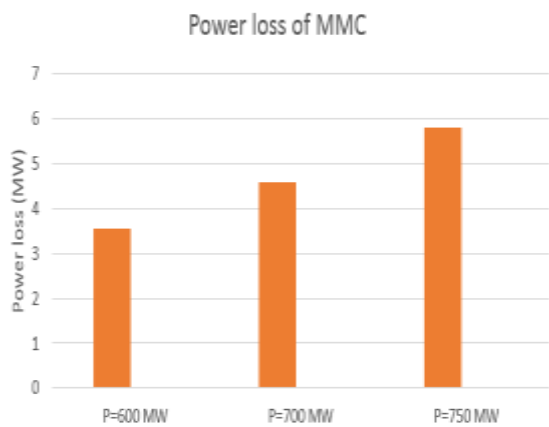


Fig. 24. The power loss of MMC at different active powers.

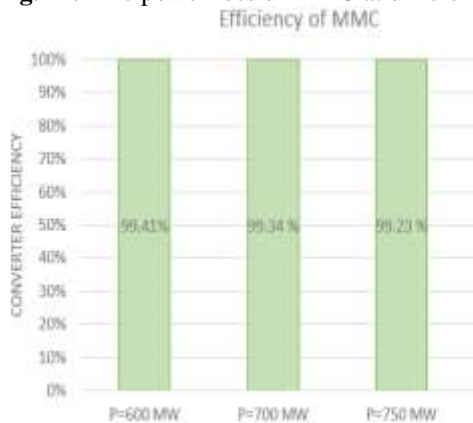


Fig. 25. The efficiency of the MMC.

Fig 24 shows the total power loss of the MMC at different active power, P=600 MW, P=700MW, and P=750MW, transmission between AC and DC networks. Fig 25 illustrates the efficiency of the MMC when it delivers different active power from the AC network to the DC distribution network.

4. Conclusion

Our main focus in this article is on the power losses related to the semiconductor devices found in MMC's submodules. The power loss classification of the MMC is explained in detail along with its mathematical modeling. To analyze the power losses associated with the devices of the submodule, a simulation platform for the power electronics system PLECS has been used. For theoretical analysis of the conduction and switching power losses of the IGBT and diodes of a submodule are carried out in MATLAB to analyze the loss characteristics of the IGBT and free-wheeling diode of a cell when switching frequency, modulation index, and power factor of the system is changed. The modular multilevel converter has been examined for the four-quadrant operations. Inverter and rectifier modes, as well as leading and lagging power factors have been considered. The most evident fact is that the various operations involve different converter losses. Focusing on the inverter and rectifier modes keeping the reactive power equal to zero (Figures 16, 17, 18, and 19), the increase of the active power flow between the converter and its ac grid increases the ac and dc currents that flow on the converter arms. As a consequence, it increases the overall conduction losses that are being generated. In general, the losses generated in the inverter and rectifier modes are quite similar to each other, but it is possible to notice that if in the

inverter mode the arm currents flow mainly in the IGBTs, in the rectifier mode the diodes are more stressed. The switching losses are strongly influenced by the reactive power injection. Increasing the reactive power injection increases the total power losses of the converter since the submodules are turned on more frequently. Moreover, there is a substantial difference between the capacitive reactive power injection and the inductive one. In the case of inductive reactive power flow between the converter and the ac grid, the switching losses are higher. Analyzing the nature of the power factors, it has been found that a reduction of the power factors entails an increase in the total converter power losses. The same considerations above can be done about inverter (I, IV) and rectifier (II, III) modes and it is also highlighted that there is a power loss asymmetry over the upper/lower switches of the submodule.

References

- [1] H. A. Pereira, V. F. Mendes, L. Harnefors and R. Teodorescu, "Comparison of 2L-VSC and MMC-based HVDC Converters: Grid Frequency Support Considering Reduced Wind Power Plants Models," *Electric Power Components and Systems*, vol. 45, pp. 2007-2016, 2017.
- [2] Á. Espín-Delgado, S. Rönnerberg, T. Busatto, V. Ravindran and M. Bollen, "Summation law for supraharmmonic currents (2--150 kHz) in low-voltage installations," *Electric Power Systems Research*, vol. 184, p. 106325, 2020.
- [3] M. Ji, Y. Wang, K. Tan and C. Wang, "A voltage-balanced hybrid MMC topology for DC fault ride-through," in *2019 IEEE Innovative Smart Grid Technologies-Asia (ISGT Asia)*, 2019.
- [4] X. Yang, Y. Xue, B. Chen, Z. Lin, Y. Mu, T. Q. Zheng, S. Igarashi and Y. Li, "An enhanced reverse blocking MMC with DC fault handling capability for HVDC applications," *Electric Power Systems Research*, vol. 163, pp. 706-714, 2018.
- [5] A. Al Hadi, X. Fu and R. Chaloo, "IGBT module loss calculation and thermal resistance estimation for a grid-connected multilevel converter," in *Wide Bandgap Power and Energy Devices and Applications III*, 2018.
- [6] Z. Rymarski, K. Bernacki and Ł. Dyga, "Measuring the power conversion losses in voltage source inverters," *AEU-International Journal of Electronics and Communications*, vol. 124, p. 153359, 2020.
- [7] R. Marquardt, "Stromrichterschaltung mit verteilten Energiespeichern und Verfahren zur Steuerung einer derartigen Stromrichterschaltung," *Patentschrift DE 101 03 031 B4*, 2001.
- [8] A. A. Mahmoud, A. A. Hafez and A. M. Yousef, "Modular Multilevel Converters for Renewable Energies Interfacing: Comparative review," in *2019*

IEEE Conference on Power Electronics and Renewable Energy (CPERE), 2019.

- [9] J. Zhu, T. Wei, Q. Huo and J. Yin, "A full-bridge director switches based multilevel converter with DC fault blocking capability and its predictive control strategy," *Energies*, vol. 12, p. 91, 2019.
- [10] M. A. Perez, S. Bernet, J. Rodriguez, S. Kouro and R. Lizana, "Circuit topologies, modeling, control schemes, and applications of modular multilevel converters," *IEEE transactions on power electronics*, vol. 30, pp. 4-17, 2019.
- [11] M. Ahmadijokani, M. Mehrasa, M. Sleiman, M. Sharifzadeh, A. Sheikholeslami and K. Al-Haddad, "A back-stepping control method for modular multilevel converters," *IEEE Transactions on Industrial Electronics*, vol. 68, pp. 443-453, 2020.
- [12] Y. Parag and M. Ainspan, "Sustainable microgrids: Economic, environmental and social costs and benefits of microgrid deployment," *Energy for Sustainable Development*, vol. 52, pp. 72-81, 2019.
- [13] Y. Dong, H. Yang, W. Li and X. He, "Neutral-point-shift-based active thermal control for a modular multilevel converter under a single-phase-to-ground fault," *IEEE Transactions on Industrial Electronics*, vol. 66, pp. 2474-2484, 2018.
- [14] H. Makhameh, M. Sleiman, O. Kükrer and K. Al-Haddad, "Lyapunov-based model predictive control of a PUC7 grid-connected multilevel inverter," *IEEE Transactions on Industrial Electronics*, vol. 66, pp. 7012-7021, 2018.
- [15] M. Sleiman, K. Al-Haddad, H. F. Blanchette and H. Y. Kanaan, "Insertion index generation method using available leg-average voltage to control modular multilevel converters," *IEEE Transactions on Industrial Electronics*, vol. 65, pp. 6206-6216, 2017.
- [16] S. Arazm and K. Al-Haddad, "ZPUC: A new configuration of single DC source for modular multilevel converter applications," *IEEE Open Journal of the Industrial Electronics Society*, vol. 1, pp. 97-113, 2020.
- [17] X. Li, B. Zhao, Y. Wei, X. Xie, Y. Hu and D. Shu, "DC fault current limiting effect of MMC submodule capacitors," *International Journal of Electrical Power & Energy Systems*, vol. 115, p. 105444, 2020.
- [18] A. Shekhar, T. B. Soeiro, Z. Qin, L. Ramírez-Elizondo and P. Bauer, "Suitable Submodule Switch Rating for Medium Voltage Modular Multilevel Converter Design," *2018 IEEE Energy Conversion Congress and Exposition (ECCE)*, 2018.
- [19] Y. Tian, H. R. Wickramasinghe, J. Pou and G. Konstantinou, "Loss distribution and characterization of MMC sub-modules for HVDC applications," *International Transactions on Electrical Energy Systems*, vol. 31, p. e13042, 2021.
- [20] Y. Tian, H. R. Wickramasinghe, P. Sun, Z. Li, J. Pou and G. Konstantinou, "Assessment of Low-Loss Configurations for Efficiency Improvement in Hybrid Modular Multilevel Converters," *IEEE Access*, vol. 9, pp. 158155-158166, 2021.
- [21] Panneerselvam, Sivaraj, and Baskar Srinivasan. "Switching loss analysis of IGBT and MOSFET in single phase PWM inverter fed from photovoltaic energy sources for smart cities." *International Journal of System Assurance Engineering and Management* 13, 2022.
- [22] Y. Tian, H. R. Wickramasinghe, Z. Li, J. Pou and Georgios Konstantinou, "Review, classification and loss comparison of modular multilevel converter submodules for HVDC applications." *Energies* 15.6, 2022.